The Rate of Isothermal Hydration of Polyperfluorosulfonic Acid Membranes

by

Trung Van Nguyen *
Department of Chemical and Petroleum Engineering
4006 Learned Hall
The University of Kansas
Lawrence, Kansas 66045-2223

and

Nicholas Vanderborgh
Los Alamos National Laboratory
Los Alamos, NM 87545

Submitted as a research paper to the Editor of
the *Journal of Membrane Science*
Professor W. J. Koros
Chemical Engineering Department
University of Texas
Austin, TX 78712-1062

First Submission: September 23, 1997
Revised: December 22, 1997

Key Words: Effective Diffusion Coefficient of Water in membranes, Non-Equilibrium Boundary Conditions, Dynamic Thermogravimetric Analysis, and Fuel Cells.

* To whom all correspondence should be addressed.

Abstract

Water transport rates through polyperfluorosulfonic acid membranes at relatively low water content (close to the fuel cell failure mode) were investigated using dynamic thermogravimetry. A model was developed to describe water transport within the membrane during the dynamic thermogravimetry experiment. Using the model, the experimental data, and a nonlinear regression technique, values for the effective diffusion coefficient of water in the Dow Chemical Company's experimental membrane samples of the same equivalent weight but of two different thickness, 10.16 μm and 17.78 μm, were obtained for temperatures of 60°C, 80°C, and 90°C. Results show that the effective diffusion coefficient of water in the membrane increases with water content and temperature. Values for the partition coefficient of water in these membranes at these temperatures are determined and found to be in close agreement with published values. Finally, rehydration of polyperfluorosulfonic acid membranes is found to be controlled by both the gas/solid interface and the diffusion of water into the inner structure of the membrane.

Introduction

Fuel cells and batteries require components (electrolytes/separators) that exhibit high ionic conductivity to separate the anodic and cathodic zones. Early hydrogen-oxygen fuel cells used a separator filled with an aqueous solution, such as potassium hydroxide, sulfuric acid or phosphoric acid, for this purpose. However, very thin (so-called “zero gap”) designs necessary to minimize ionic resistance require more restricted mixing between the anode and cathode compartments. Ion exchange polymeric membranes are now used successfully for this purpose [1].

The first polymeric membrane separators were fabricated with technical polymers such as sulfonated polystyrene. However, chemical stability and thermal stability requirements led to the introduction of polyperfluorosulfonic acid polymers, typified by the Nafion® class of

polymers, marketed by the DuPont Company [2]. During the last years, the Dow Chemical Company introduced new polyperfluorosulfonic acid (PFSA) materials [3] with improved chemical and physical properties [4]. Ion transport through these membranes involves both proton migration between adjacent sulfonic acid-anionic sites and water dynamics within these materials. At one extreme, low water content, the polymers exhibit only limited ionic conductivity. As water content increases, conductivity generally increases into regimes that can surpass similar ionic solutions. There is a general understanding that these polymer formulations partition volume between ionic and polymeric domains, and that the ionic domains exhibit a considerable degree of structure [5]. In the extreme case, spectroscopic data on dried polymer samples containing metallic ions, such as silver, suggest periodically ordered ionic clusters containing approximately 50 anion-cation ion pairs [6,7]. The extent of order is less in water-filled (equilibrated in liquid water) polymers or in materials of lower equivalent weight.

These membranes have proven their usefulness in the production of caustic and chlorine from NaCl solutions. During this process the membrane is submerged in aqueous electrolyte and considerable water invades the membrane matrix. Fuel-cell operation involves using the membrane suspended in flowing gaseous mixtures. One well-known fuel-cell failure mechanism is membrane dehydration that results in sharply lower ionic conductivity. This condition can be caused by excessive operating temperatures, insufficient water content of the feed gases, or excessive current densities that can result from high localized temperatures or nonuniform water distribution within the membrane. Restoration of conductivity requires water transport from the gas phase into the membrane or back-diffusion of water produced at the cathode to increase membrane water content [8]. The study of this process, gas-phase water transport into a partially dry membrane and water transport across a membrane suspended in humidified gaseous streams, is the focus of the work described here in this paper. Experimental PFSA membranes from the Dow Chemical Company were used in this study.

Experimental

This work studies polyperfluorosulfonic acid membranes in equilibrium with various water containing gas streams. An experimental technique called Dynamic Thermogravimetry was used to study water transport into a partially dried membrane (a process known as rehydration). Figure 1 illustrates a schematic of the apparatus employed in the experiment and a typical three-phase analysis sequence. The three-phase analysis consists of an initial drying step in which dry gas is passed over the membrane sample that is suspended in the thermo-balance. (A wire frame is used to hold the membrane sample in place and to prevent the membrane sample from coiling during the drying process.) During this time, the sample temperature is slowly increased to the measurement temperature of the second phase.

At the beginning of the second phase, termed the “isothermal water absorption step,” the dry carrier gas is switched to the humidified gas and water begins to enter the polymer from the gas phase. (A delay of a minute was allowed at the beginning of Phase 2 to account for any delay in the flow system. This was considered more than sufficient considering the average gas residence time in sample chamber is around 30 seconds or less at the gas flow rate used.) The weight of the sample is continuously monitored, plotted, and stored. The humidified gas enters the sample chamber at the same “isothermal” temperature. Next, the carrier gas is switched back to the dry gas stream for the third phase of the analysis. During this phase, the sample is heated to 180^{o}C, under nitrogen, and maintained at this temperature for 30 min. The polymer mass after this treatment is termed the “dry polymer weight.” (At 180^{o}C and a nitrogen purge, the polymer weight becomes constant---weight losses are less than 1 μg/min. At higher temperatures, higher rates of weight loss suggest polymer degradation. At lower temperatures, residual quantities of water are only slowly removed.) Thus this procedure measures the dry polymer mass, the quantity of water in the polymer in equilibrium with a gas of known water content and temperature, and the dynamics of water addition at that temperature.

Table I shows conditions for the three phases of a typical polymer hydration dynamic experiment. Measurements were made using a TA3000 Mettler thermal analysis system. Nitrogen was used as the carrier gas along with controlled quantities of water vapor that were established by a dual series sparging system. Water vapor content in the humidified gas was periodically monitored using water absorbing material. Measuring the water content involved monitoring the flow rate of the dry gas (metered using a Tylan mass flow controller) and the weight of absorbed water. For these studies, a water content in the vapor phase of 3.65 mole percent was used. The flow rate of the carrier gas was 200 STP cc/min. The water flow rate in the gas phase at this carrier gas flow rate and water content is approximately 40-45 times the water absorption rate of the membrane samples used in the experiments. This was done to ensure that the concentration of water in the gas phase next to the membrane is uniform and constant with time. Temperature was calibrated using features supplied with the instrument. A second temperature reading was provided by a thermocouple positioned close to the polymer sample.

Data presented here were obtained using experimental polymer samples supplied by the Dow Chemical Company. These membranes are polyperfluorosulfonic acid polymers with an equivalent weight of approximately 800. They are similar to more familiar (DuPont Company) Nafion® polymers, but are formulated with a fluorinated side chain with fewer carbon atoms than Nafion®. The membranes are assumed to be chemically homogeneous through their cross-sections and were selected to be free from pin-holes and other discontinuities. The membranes received were pretreated to convert them to the proton form used in these studies. This pretreatment involved the following steps: boil in 1M HNO_3 for 1 hour; cool slowly to avoid tearing; rinse thoroughly with deionized water; autoclave in deionized water at a temperature of 120^{o}C for one hour; rinse in deionized water; and store in deionized water. Following these steps, the membrane samples were essentially transparent.

Each experiment involved mounting a membrane approximately 1 cm by 2 cm on a membrane holder connected to the hang-down assembly in the microbalance. The membranes reported here had equivalent weights of approximately 800, dry density of 2.0 g/cm^3, and two different thickness (dry measurement), 10.16 μm and 17.78 μm, respectively. Experiments were conducted for each sample at three temperatures, 60^{o}C, 80^{o}C, and 90^{o}C.

Results and Discussion

Thermogravimetric Experiments

These experiments are designed to measure the rate of water transport within the membranes at low water content (2 to 3 water molecules per sulfonic acid site), i.e., the process of rehydration of a membrane. Previous studies show that conductivity is restricted when water contents fall below an average of 2 water molecules per sulfonic acid site [9]. Thus, drying and rewetting cover exactly this water concentration regime where performance loss is observed. Other technologies that use these membranes, such as electrosynthesis, operate with far higher water content. Figure 2 shows results from Phase 2 of a typical dynamic thermodynamic experimental run. Note that both data of the weight and the rate of weight change as a function of time are given. The data of most interest are the weight of the membrane sample as a function of time during Phase 2 of the analysis, the equilibrium weight at the end of Phase 2, and the dry weight of the sample. The dry weight is needed to calculate the water contents in the membrane under any set of conditions. By knowing the equilibrium weight and the dry weight of the membrane we can also calculate the partition coefficient of water for these membranes at the testing temperature. Data obtained with the three membrane samples are shown in Table II.

These results given in Table II were used to calculate values for the partition coefficient of water in the membrane, K_w [10], defined as,

$$K_w(T) = \frac{c_{w,eq}}{P_w} \equiv \quad \text{(mol } H_2O/cm^3 \text{ dry membrane volume-atm)} \qquad [1]$$

where $c_{w,eq}$ and P_w are the concentration of water in the membrane at equilibrium and the partial pressure of water in the gas phase, respectively. Table III presents values for the partition coefficient of water for the two polymer samples of the same equivalent weight. As is apparent, the samples show similar characteristics within this temperature range. Results were reproducible to within 5 percent. For comparison purpose, corresponding number of water molecules per sulfonic site and water activity (P_w/P_{sat}) are also included along with the results from Morris and Sun [11] and Hinatsu *et al* [12] for Nafion 117 and Zawodzinski *et al* [4] for DOW XUS 13204.10 at similar conditions. Note that our values are very close to that of reference 11.

Water Transport Model for Parametric Analysis

A model of water transport in a membrane was developed for two purposes: 1) to achieve insight into water transport from the gas phase into a partially dried membrane, especially transport through the surface layer, and how the polymer structure changes during this process; and 2) to obtain values for the diffusion coefficient of water in these polyperfluorosulfonic acid membranes. In this study, the membrane/water system is assumed to be a pseudo-homogeneous medium with water transport limited to through-the-thickness (x-direction). The assumption of one dimensional water transport is based on the fact that water transport from the gas phase is uniformly distributed over the membrane surface. The membrane thickness (10.16 μm to 17.78 μm) is much smaller than the width or the length of the membrane (1 cm by 2 cm). The membrane sample was mounted so that the surface of the membrane was continuously exposed to the flowing humidified gas stream. By taking advantage of the symmetry condition at the center of the membrane and assuming

homogeneous polymer properties, only half of the membrane thickness needs to be modeled. Figure 3 shows a schematic of the modeled membrane region.

The material balance equation for water concentration within the membrane is,

$$\frac{\partial c}{\partial t} = \frac{\partial}{\partial x}\left(D(c) \frac{\partial c}{\partial x} \right) \qquad [2]$$

An exponential expression similar to that proposed by Gardner and Mayhugh [13] and later confirmed by others [14] to describe the water content dependence of the diffusivity of water in porous media was found to provide the best fit to the experimental data:

$$D = D^* e^{(mc)} \qquad [3]$$

where the parameters D^* and m are empirical constants. The diffusion coefficient used here represents the effective water diffusion coefficient through the range of water contents of interest. Because the membrane is treated as a pseudo-homogeneous medium, the effective diffusion coefficient includes all the morphological properties of the membrane. Units for water concentration in the membrane are moles of water per unit volume (cm^3) of dry polymer. The volume change as a result of membrane swelling when water contents change through the ranges studied here is small (no more than 4 percent in these experiments) and can be neglected.

The initial and boundary conditions used are,

at t=0, $c = c_{init}$ *[4]*

at t>0 and x=0, $c = c_{ini} + (c_{eq} - c_{init}) e^{(-k/t)}$ *(gas/membrane interface)* *[5]*

at t>0 and x=l/2, $\frac{\partial c}{\partial x} = 0$ *(symmetry condition)* *[6]*

where *l* is the thickness of the membrane; c_{eq} is the equilibrium (uniform) water concentration obtained at the end of Phase 2; c_{init} is the initial water concentration in the membrane at the beginning of Phase 2; and the empirical parameter *k* is used to describe the non-equilibrium boundary condition at the membrane/gas interface. The boundary condition used at the gas and membrane interface *(x=0)* was chosen after detailed data analysis of the initial results. This boundary condition is necessary to account for the resistance to mass transport through the surface in contact with the humidified gaseous stream. Water concentration at the membrane surface does not reach equilibrium values instantaneously. Rather, this process requires considerable time (several tens of seconds) following the switch between dry (phase 1) and humidified (phase 2) gas. Note that when *t* in Eq. [5] is very small, *c* is equal to c_{ini} , and for large *t* values, *c* approaches c_{eq}.

The skin effect can be also illustrated by considering simulated data showing sample weight and weight gain rate during an absorption experiment. These data are given in Figure 4 for four different cases. In case 1, the concentration of the absorbate at the sample interface is assumed to be in equilibrium immediately with its concentration in the gas phase (i.e., when *k*=0, $c_{interface} = c_{eq}$). In case 2, a non-equilibrium boundary condition (Eq. [5]) was modeled to account for the delay in reaching equilibrium. A value of 30s was used for *k,* and other conditions are the same as in case 1. In case 3, *k*=60s was used to illustrate the effect of an even longer delay constant. (Other conditions are identical to cases 1 and 2.) In case 4, in addition to *k*=30s as in case 2, the water diffusion coefficient was increased by a factor of four. Note that for case 1, there was no visible delay and the sample weight increased continuously until it reached an equilibrium amount. The other simulated curves clearly show slower weight gain, which increases with higher *k* value. Furthermore, the weights of the samples increased at

a more gradual rate than that of case 1. Case 4 was included to show that the value of diffusion coefficient also affects both the shape of the curve and the duration of the delay.

The nature of kinetics during water uptake is also illustrated when the rate of weight gain, rather than the sample weight, was plotted against time (Figure 5). In the instantaneous equilibrium case (Case 4), the weight gain rate begins at a maximum value and decreases continuously from there. For the other three cases, the weight gain rate begins at a far lower value, increases until it reaches a maximum, and decreases continuously after that. The locations of the maximum weight gain were determined by the values of the parameter *k* and the diffusion coefficient of the absorbate. Higher diffusion coefficients are shown to raise the maxima and shift the location of the maxima to the left.

Consequently, if results display the same behavior as shown in Figure 5 (see actual results shown in Figure 2) even after sufficient time occurred to account for the gas-switch-over delay, this indicates a non-equilibrium condition at the membrane and humidified gas interface. This use of the weight gain rate data to indicate a non-equilibrium condition at the interface has not been shown previously. However, Dovi *et al.* [15] showed the importance of setting the correct boundary conditions in the estimation of diffusion coefficients from sorption experiments. In their work, the more gradual increase in the sample weight was used as the indicator to describe this phenomenon of higher surface resistance.

Finally, the experiments were conducted in a way that the effect of water transport within the gas phase can be neglected. Sufficiently high water flow rate in the gas phase (40-45 times the water absorption rate of the samples) was set to ensure that the gas phase water concentration at the membrane surface is constant with time. These precautions were used to ensure that the transport phenomenon shown here was that of water in the membrane with minimal effects from the gas phase composition. With the precautions above and the fact that the diffusivity of water in the gas phase is at least four orders of magnitude higher than in the

membrane, one can rule out the chance that the gas boundary layer at the membrane surface is a limiting factor.

The model equations were cast in finite difference form and solved numerically because the model is nonlinear. Values for the parameters were obtained using the IMSL nonlinear least-square regression subroutine UNLSF [16] and the following objective function:

$$F = \sum_{j=1}^{ne} [w_{\exp}(t_j) - w_{pred}(t_j)]^2 \qquad [7]$$

where w_{exp} *and* w_{pred} are the experimental and model predicted total weight of the membrane sample, respectively; and *ne* is the number of data points used in the analysis and

$$w_{pred}(t_j) = (2)(18.016)(area)\left(\int_{x=0}^{x=l/2} c(x,t_j)dx\right) + w_{dry} \qquad [8]$$

where w_{dry} and *Area* denote the dry weight of the sample and the dry cross sectional area of the membrane sample, respectively.

The fitting parameters were the water adsorption time delay constant for the polymer, *k*, and the two parameters of the effective diffusion coefficient of water, D^* and *m*, respectively. The model was fitted to the total sample weight for both membrane thicknesses measured at various times during Phase 2 of the experiment. This process was repeated for each of three temperatures (60°C, 80°C, and 90°C).

Figures 6 and 7 show the comparison between the predicted results using this model and the experimental data obtained with the 10.16-mm and 17.78-mm membrane samples at three temperatures, 60°C, 80°C, and 90°C. The model described the experimental data reasonably well. Table IV shows values for the parameters *k,* D^**,* and *m* for these low-water-content polymer samples, and Figure 8 shows the behavior of the effective water diffusion

coefficient in the membrane samples, through the range of water contents and at the three temperatures investigated here. Values for the 17.78-μm membrane appear slightly higher than those for the 10.16-μm membrane at all temperatures. However, since the differences are still within experimental errors, we could not rule out the assumption that they have similar bulk properties. Future studies at higher water content will reveal any differences between these two materials. For comparison purpose, values for Nafion® 117 and DOW XUS 13204.10 membranes from other sources [4,11,17] are also included in Figure 8. Data from references 4 and 17 were obtained by pulsed field gradient spin-echo 1H NMR, and those from reference 11 were obtained by the Cahn microbalance method. Note that the values obtained here are closer to those reported in reference 11 than those in references 4 and 17. The high values reported in references 4 and 17 might be attributed to the questionable assumption made by the authors that water and H^+ diffuse by an identical mechanism at low water content.

Finally, the effective diffusion coefficient of water in these membranes was observed to increase significantly with increasing water content and temperature. These observations are interpreted as the result of water invading and expanding collapsed gel-like network. Water occupies specific sites in the ionic domains, in close proximity to the sulfonic acid moieties. The reconnection of the network, coupled to an increase in transport area resulting from swelling, leads to increasing water transport rates. At levels near one molecule of water per sulfonic acid site, the polymer structure exhibits water transport rates that are insensitive to temperature (Figure 8). The activation energy for water diffusion obtained for the Dow Company membrane in this work is approximately 28.4 kJ/mol, which is close to values reported by Yeo and Eisenberg (20.2 kJ/mol) [18] and Morris and Sun (23 kJ/mol) [10] for Nafion®. Table IV also shows that values for the parameter *k* termed the ``absorption equilibrium delay constant'' for the two thickness, decrease with increasing temperature. A decrease in the value of the

parameter *k* indicates a shorter time for an equilibrium state between the water at the membrane surface and the water in the gas phase.

Finally, this model permits the study of dynamic behavior of water distribution within the membrane during the rehydration events. Figure 9 shows the water distribution as a function of time within the 10.16-mm membrane at 90^{o}C. During rehydration, water transport through the membrane is controlled both by the slow equilibrium process at the membrane and gas interface and the diffusion of water into the inner structure of the membrane. As the membrane becomes hydrated, water moves through the membrane even more rapidly because of faster transport in already hydrated layers than in the drier interior. Polymer samples dried to levels below two H_2O molecules per sulfonic acid site show severely restricted water transport. Conductivity results show this restriction to be reflected in proton transport as well [9].

There has been considerable speculation on the nature of the changes that result from dehydration of these polymers [9]. FTIR surface spectroscopy studies during the drying process show migration of the sulfonic acid group away from the surface, moving into the TFE backbone phase. This result suggests that the hydronium-sulfonate (one molecule of water/site) moiety does not partition into an “aqueous phase.” Thus the polymer network collapses during complete dehydration. Adding water into the collapsed network is restricted because the sulfonic acid sites are no longer accessible. These data show appreciable time is required to restructure the network. Obviously, volume change occurs during that water addition process.

Conclusions

A dynamic thermogravimetric experiment was conducted to study the transport of water into controlled water content polyperfluorosulfonic acid membranes (a process known as rehydration) at 60^{o}C, 80^{o}C, and 90^{o}C. The membranes studied were manufactured by the Dow Chemical Company, with two different thickness but the same equivalent weight. A mathematical model of water transport in a membrane was developed to analyze the hydration

data and determine the effective water diffusion coefficient in these membranes. The effective diffusion coefficient of water was observed to increase with the increase in temperature and water content in the membrane. The dependence of the diffusion coefficient of water on temperature was also determined. Finally, it was found that rehydration of polyperfluorosulfonic acid membranes was controlled by both the gas/solid interface and the diffusion of water into the collapsed inner structure of the membrane.

The results obtained from this work suggest failure mechanisms within working fuel cells that use polyperfluorosulfonic acid membranes as the electrolyte. Membranes that are dried, and thus form zones with limited water transport, can remain in failure modes. Rehydration, where possible, is a slow process, especially for the initial stages in which maximum network collapse occurs. Rehydration is considerably accelerated at higher temperatures. Obviously, control systems must function to sustain hydration content at higher than critical levels. Finally, values for the partition coefficient of water in these membranes within these temperatures were also determined.

Acknowledgment

We wish to thank Mr. Joseph Guante, LANL, for assisting with the thermogravimetric experiment and the Dow Chemical Company for providing us the membrane samples.

List of symbols

Area	Dry cross-sectional area of the membrane sample, cm^2.
c, c_w	Concentration of water in the membrane, mol/cm^3 dry volume.
c_{eq}	Concentration of water in the membrane at equilibrium, mol/cm^3 dry volume.
c_{ini}	Initial concentration of water in the membrane, mol/cm^3 dry volume.
D(c)	Effective diffusivity of water in the membrane, cm^2/s.
D^*	Empirically fitted parameter in Equation [3], cm^2/s.
dWt/dt	Weight gain rate of the membrane, g/sec.
k	Adsorption rate of water for 2.5 mil membrane, sec.
K_w	Partition coefficient of water in the membrane, mol H_2O/cm^3 of dry volume-atm.
l	Thickness of the membrane, cm.
m	Empirical constant used in the expression of the diffusivity of water, cm^3 dry volume/mol.
ne	Number of data points used in the parametric analysis.
P_w	Partial pressure of water, atm.
t	Time, sec.
x	x-coordinate along the thickness of the membrane, cm.
w_{dry}	Experimental value of the dry weight of the sample, g.
w_{exp}	Experimental value of the total weight of the sample, g.
w_{pred}	Predicted value of the total weight of the sample, g.

References

1. G.A. Eisman, “The Application of a New Perfluorosulfonic Acid Ionomer in Proton-Exchange Membrane Fuel Cells: New Ultra-high Current Density Capabilities,“ in Fuel Cell Technology and Applications, PED Management Office for Energy Research, the Netherlands, 1987, p. 287.

2. W.G.F. Grot, G.E. Munn and P.N. Walmsley, “Perfluorinated Ion Exchange Membranes,” 141th National Meeting, The Electrochemical Society, Houston, Texas, May 7-11 (1972).

3. B.R. Ezzell, W.P. Carl and W.A. Mod, “Ion Exchange Membranes for the Chlor-Alkali Industry,” in Industrial Membrane Processes, R. E. White and P. N. Pintauro, Eds., AIChE Symposium Series, **82**, (1986) 45.

4. Thomas A. Zawodzinski, Jr., Thomas E. Springer, John Davey, Roger Jestel, Cruz Lopez, Judith Valerio and Shimshon Gottesfeld, “A Comparative Study of Water Uptake by and Transport Through Ionomeric Fuel Cell Membranes,” *J. Electrochem. Soc.*, **140**, (1993) 1981.

5. K.A. Mauritz, “A Review and Critical Analysis of Theories of Polar/Nonpolar Aggregation in Ionomers,” in Structure and Properties of Ionomers, M. Pineri and A. Eisenberg, Eds., D. Reidel Publishing Company, Dordrecht, Holland, 1986, p. 11.

6. T.D. Gierke, G.E. Munn and F.C. Wilson, “The Morphology in Nafion® Perfluorinated Membrane Products, as Determined by Wide and Small Angle X-Ray Studies,” *J. Polymer Sci.*, **19**, (1981) 1687.

7. W.Y. Hsu and T.D. Gierke, “Ion Transport and Clustering in Nafion® Perfluorinated Membranes,” *J. Membrane Sci.*, **13**, (1983) 307.

8. Trung Nguyen, James Hedstrom and Nicholas Vanderborgh, “Heat and Mass Transfer Design Issues in PEM Fuel Cell Hardware,” Proceedings of the Symposium on Fuel Cells, The Electrochemical Society, Inc., Pennington, NJ, 1989.

9. P.C. Rieke and N.E. Vanderborgh, “Temperature Dependence of Water Content and Proton Conductivity in Polyperfluorosulfonic Acid Membranes,” *J. Membrane Sci.*, **32**, (1987) 313.

10. Mark W. Verbrugge and Robert F. Hill, “Ion and Solvent Transport in Ion-Exchange Membranes,” *J. Electrochem. Soc.*, **137**, (1990) 886.

11. David R. Morris and Xiaopong Sun, “Water-Sorption and Transport Properties of Nafion 117 H,” *J. Membrane Sci.*, **50**, (1993) 1445.

12. James T. Hinatsu, Minoru Mizuhata, and Hiroyasu Takenaka, “Water Uptake of Perfluorosulfonic Acid Membranes from Liquid Water and Water Vapor,” *J. Electrochem. Soc.*, **141**, (1994) 1493.

13. W.R. Gardner and M.S. Mayhugh, “Solutions and Tests of the Diffusion Equation for the Movement of Water in Soil,” *Soil Sci. Soc. Am. Proc.*, **22**, (1958) 197.

14. Bu-Xuan Wang and Zhao-Hong Fang, “Water Absorption and Measurement of the Mass Diffusivity in Porous Media,” *Int. J. Heat Mass Transfer*, **31**, (1988) 251.

15. V.G. Dovi, O. Paladino and H. Preisig, “The Importance of Correct Boundary Conditions in the Estimation of Diffusion Coefficients from Mass Sorption Experiments,” *Int. Comm. Heat Mass Transfer*, **15**, (1988) 669.

16. UNLSF Subroutine of IMSL library, in “Problem-Solving Software System for Mathematical and Statistical FORTRAN Programming,” *IMSL User’s Manual,* Version 1.0, IMSL, Inc., Houston, TX 77042 (1987).

17. Thomas A. Zawodzinski, Jr., Michal Neeman, Laurel O. Sillerud and Shimshon Gottesfeld, “Determination of Water Diffusion Coefficients in Perfluorosulfonate Ionomeric Membranes,” *J. Phys. Chem*., **95**, (1991) 6040.

18. S.C. Yeo and A. Eisenberg, “Physical Properties and Supermolecular Structure of Perfluorinated Ion-Containing (Nafion) Polymers,” *J. Appl. Polym. Sci*., **21**, (1977) 875.

List of Table Captions

I. Dynamic hydration experiment conditions for a 90^{o}C run.

II. Results from the dynamic thermogravimetric experiment.

III. Partition coefficient of water for Dow Co. polymers.

IV. Fitted values for the parameters k, D^{*}, and m.

List of Figure Captions

1. Schematic of the thermogravimetric system and a typical analysis experiment.
2. Results from a typical dynamic thermogravimetric run.
3. A schematic of the membrane modeled region.
4. Effect of boundary condition type on membrane weight during rehumidification: : (no symbol) k=0 s; (+) k=30 s; (o) k=30 s, higher D; (Δ) k=60 s.
5. Effect of boundary condition type on membrane weight gain rate during rehumidification: (no symbol) k=0 s; (+) k=30 s; (o) k=30 s, higher D; (Δ) k=60 s.
6. Comparison of predicted results from model to experimental data for Dow Co. 10.16-μm membrane at 60^{o}C, 80^{o}C, and 90^{o}C. Solid lines represent model results, and symbols represent experimental data: (+) T=60^{o}C; (o) T=80^{o}C; ($\lozenge$) T=90^{o}C.
7. Comparison of predicted results from model to experimental data for Dow Co. 17.78-μm membrane at 60^{o}C, 80^{o}C, and 90^{o}C. Solid lines represent model results, and symbols represent experimental data: (+) T=60^{o}C; (o) T=80^{o}C; ($\lozenge$) T=90^{o}C.
8. Experimentally fitted effective diffusion coefficient of water in Dow Co. membranes at 60^{o}C, 80^{o}C, and 90^{o}C. Solid lines are results for 10.16-μm membrane, and dashed lines are results for 17.78-μm membrane. ($\bullet$) Nafion 117, 50^{o}C, Ref. 11; (x) Nafion 117, 30^{o}C, Ref. 4; (+) Dow XUS 13204.10, 30^{o}C, Ref. 4; ($\lozenge$) Nafion 117, 100^{o}C, Ref. 11.
9. Predicted water distribution in the membrane as a function of time after humidified gas was introduced for 10.16-μm membrane at 90^{o}C. Each line represents a profile every 15-s interval.

Table I. Dynamic hydration experiment conditions for a 90°C run.

Carrier Gas Flow Rate:	200 STP cc/min
Water Content in Phase 2:	3.65 mol percent
Phase 1: Drying Step	
Initial Temperature:	35°C
Temperature Program Rate:	to 60°C @ 0.4 K/min
	to 80°C @ 0.8 K/min
	to 90°C @ 1.0 K/min
Gas:	Dry
Phase 2: Isothermal Absorption Step	
Temperature:	Isothermal for 30 min
Gas:	Humidified
Phase 3: Second Drying Step	
Initial Temperature:	50°C
Temperature Program Rate:	To 180°C @ 20 K/min
	Isothermal at 180°C for 30 min
Gas:	Dry

Table II. Results from the dynamic thermogravimetric experiment.

Thickness (μm)	**Temp** (^{o}C)	**MIN *** (% H_2O)	**MAX *** (% H_2O)	**Dry Wt *** (g)	**Max dWt/dt **** (g/s)
10.16	60	2.73	6.45	0.0169	3.22E-6
	80	2.63	5.14	0.0181	2.45E-6
	90	1.99	3.91	0.0181	1.65E-6
17.78	60	3.02	6.59	0.0278	3.68E-6
	80	2.49	4.77	0.0284	2.38E-6
	90	2.26	4.18	0.0286	2.12E-6

* Refer to Figure 1.

** Value from the highest slope, dWt/dt (see Figure 2).

Table III. Partition coefficient of water for Dow Company polymers.

Thickness	**K_w (mol H_2O/cm^3 dry volume-atm)**		
(μm)	60°C	80°C	90°C
	(P_w/P_{sat}=0.19)*	(P_w/P_{sat}=0.08)*	(P_w/P_{sat}=0.05)*
10.16	0.197	0.157	0.119
	(2.9 H_2O/H^+)	(2.3 H_2O/H^+)	(1.7 H_2O/H^+)
	[2.8 H_2O/H^+]#	**[1.6 H_2O/H^+]###**	
	[2.6 H_2O/H^+]##		
17.78	0.200	0.146	0.127
	(2.9 H_2O/H^+)	(2.1 H_2O/H^+)	(1.8 H_2O/H^+)

* $P_w = 0.0365$ atm

\# For Nafion 117 at 50°C and same P_w/P_{sat}, Ref. 11.

\## For Dow Dow XUS 13204.10 membrane at 30°C and same P_w/P_{sat}, Ref. 4.

\### For Nafion 117 at same temperature (80°C) and P_w/P_{sat}, Ref. 12.

Table IV. Fitted values for the parameters *k, D**, and *m*.

Temp (^oC)	***k*** (s)	***D**** (cm^2/s)	***m*** (cm^3/mol)
	10.16 μm membrane		
60	41.3	1.63E-8	447
80	29.3	6.44E-10	1210
90	26.8	2.24E-10	1820
	17.78 μm membrane		
60	43.5	2.13E-8	521
80	36.4	4.20E-9	1010
90	28.5	9.77E-10	1480

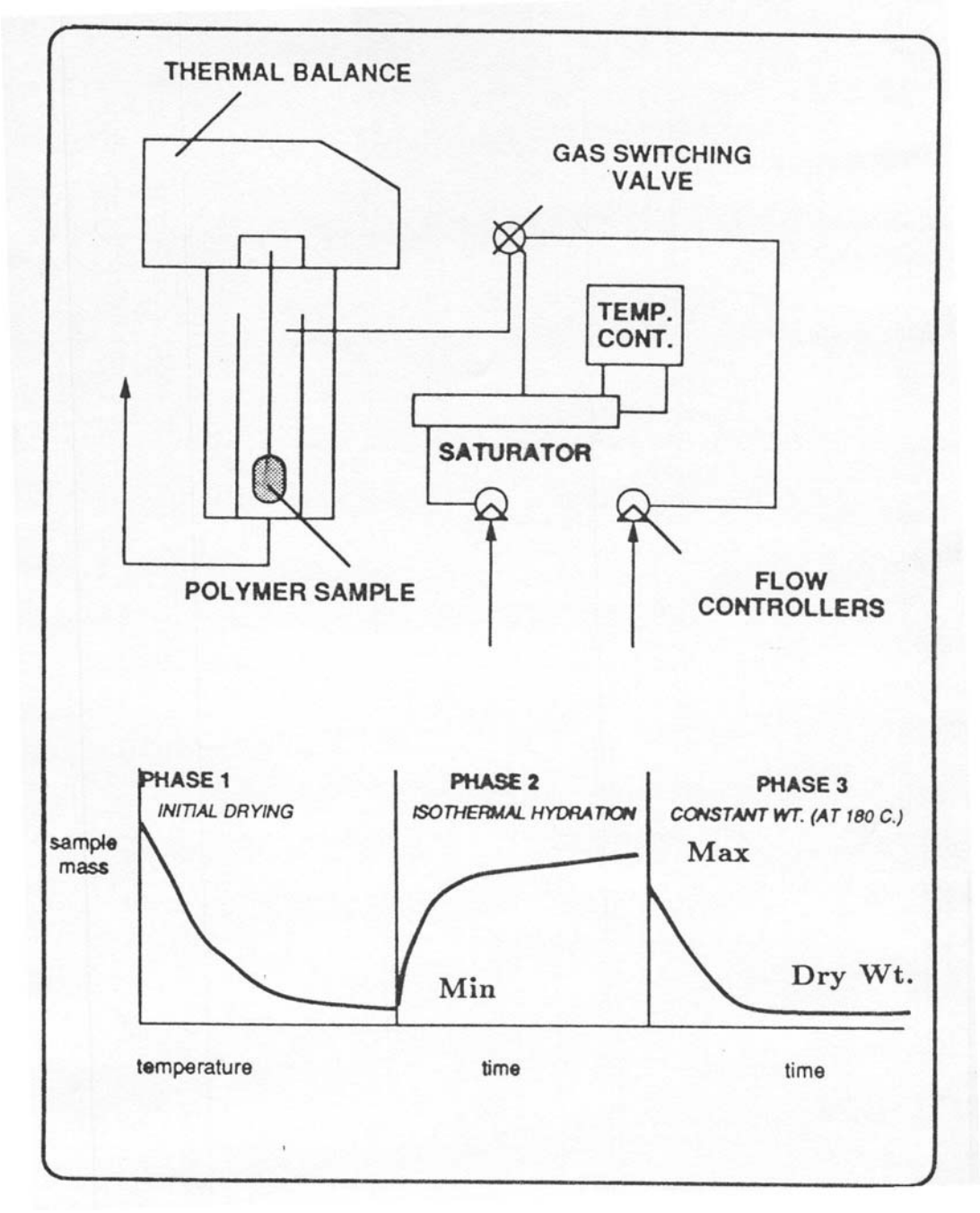

Figure 1. Schematic of the thermogravimetric system and a typical analysis experiment.

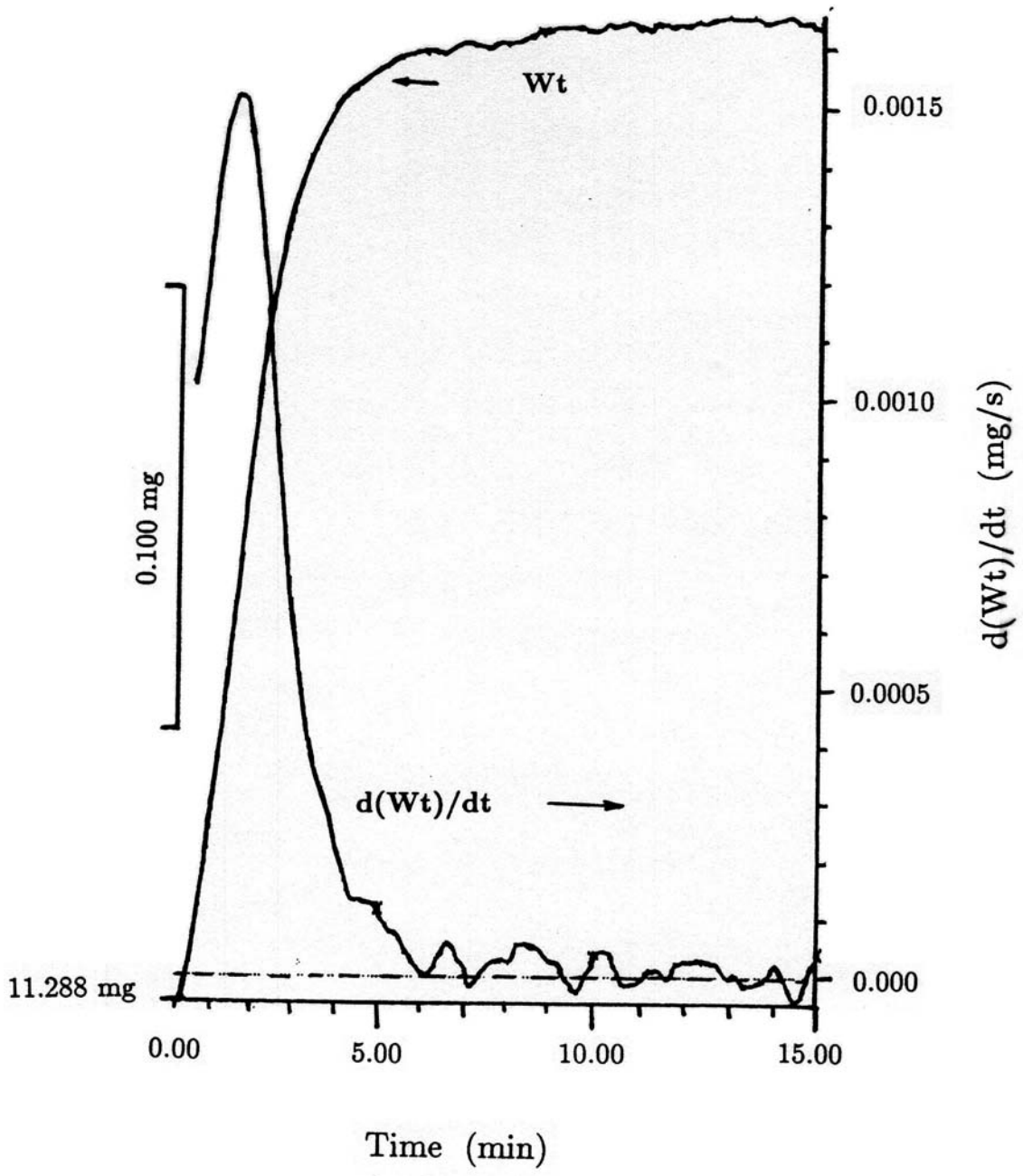

Figure 2. Results from a typical dynamic thermogravimetric run.

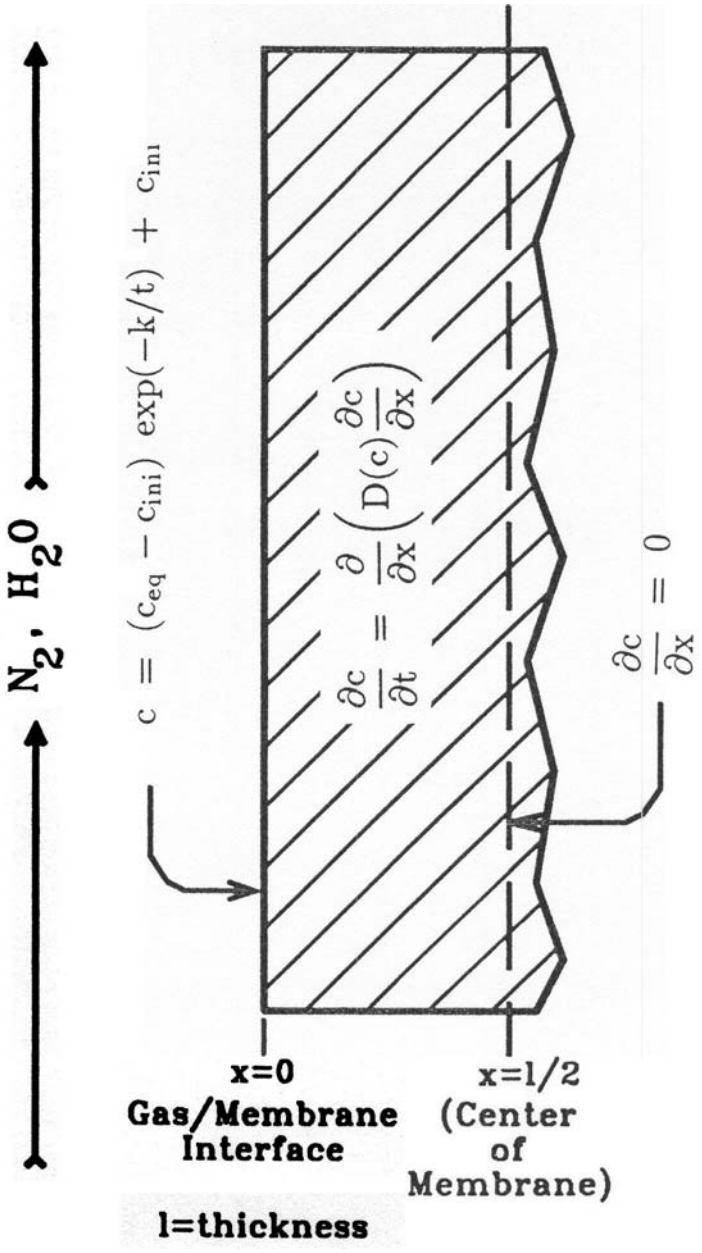

Figure 3. A schematic of the membrane modeled region.

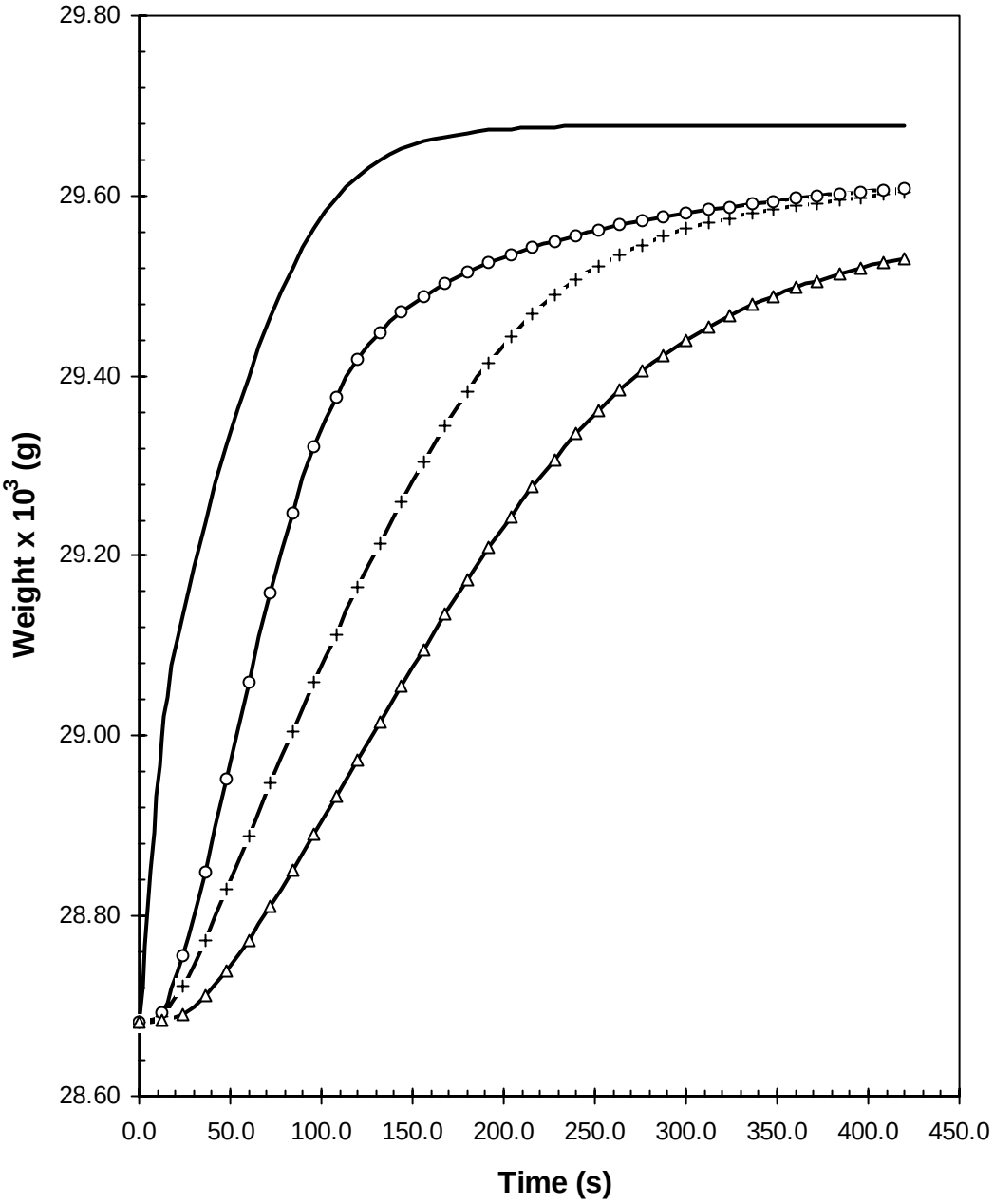

Figure 4. Effect of boundary condition type on membrane weight during rehumidification: (no symbol) k=0 s; (+) k=30 s; (o) k=30 s, higher D; (Δ) k=60 s.

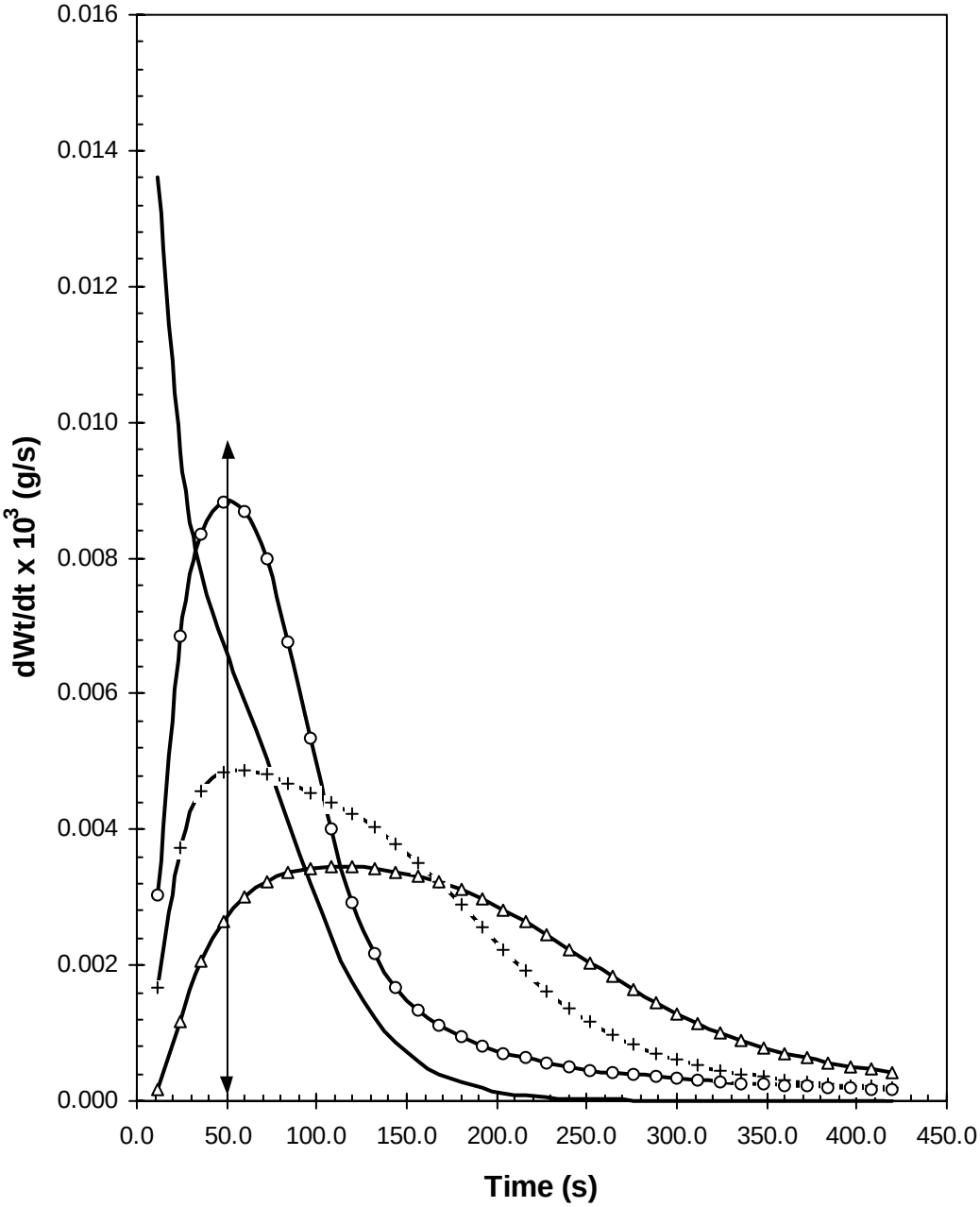

Figure 5. Effect of boundary condition type on membrane weight gain rate during rehumidification: (no symbol) k=0 s; (+) k=30 s; (o) k=30 s, higher D; (Δ) k=60 s.

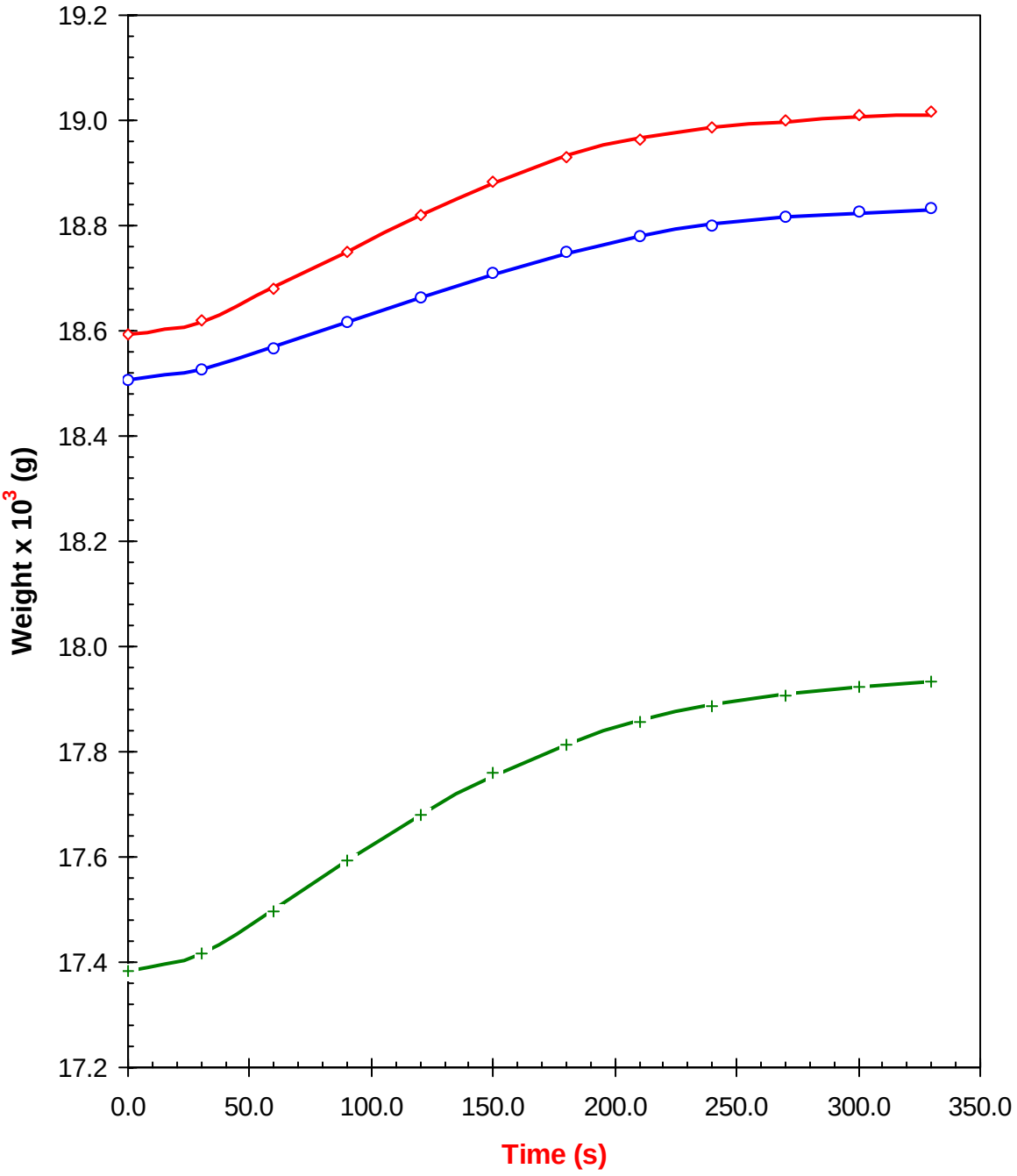

Figure 6. Comparison of predicted results from model to experimental data for Dow Co. 10.16-μm membrane at 60°C, 80°C, and 90°C. Solid lines represent model results, and symbols represent experimental data: (+) T=60°C; (o) T=80°C; (◊) T=90°C.

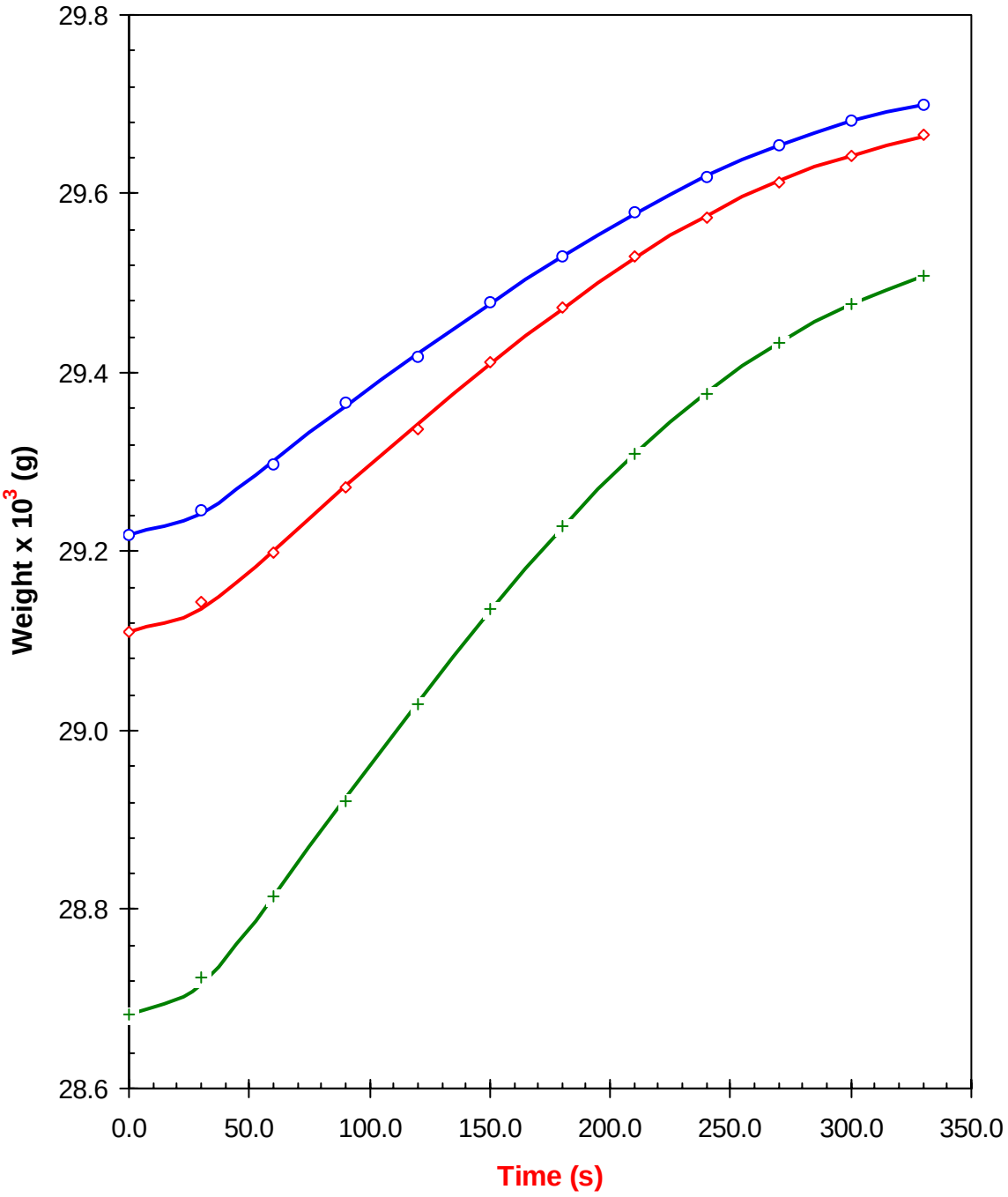

Figure 7. Comparison of predicted results from model to experimental data for Dow Co. 17.78-μm membrane at 60°C, 80°C, and 90°C. Solid lines represent model results, and symbols represent experimental data: (+) T=60°C; (o) T=80°C; (◊) T=90°C.

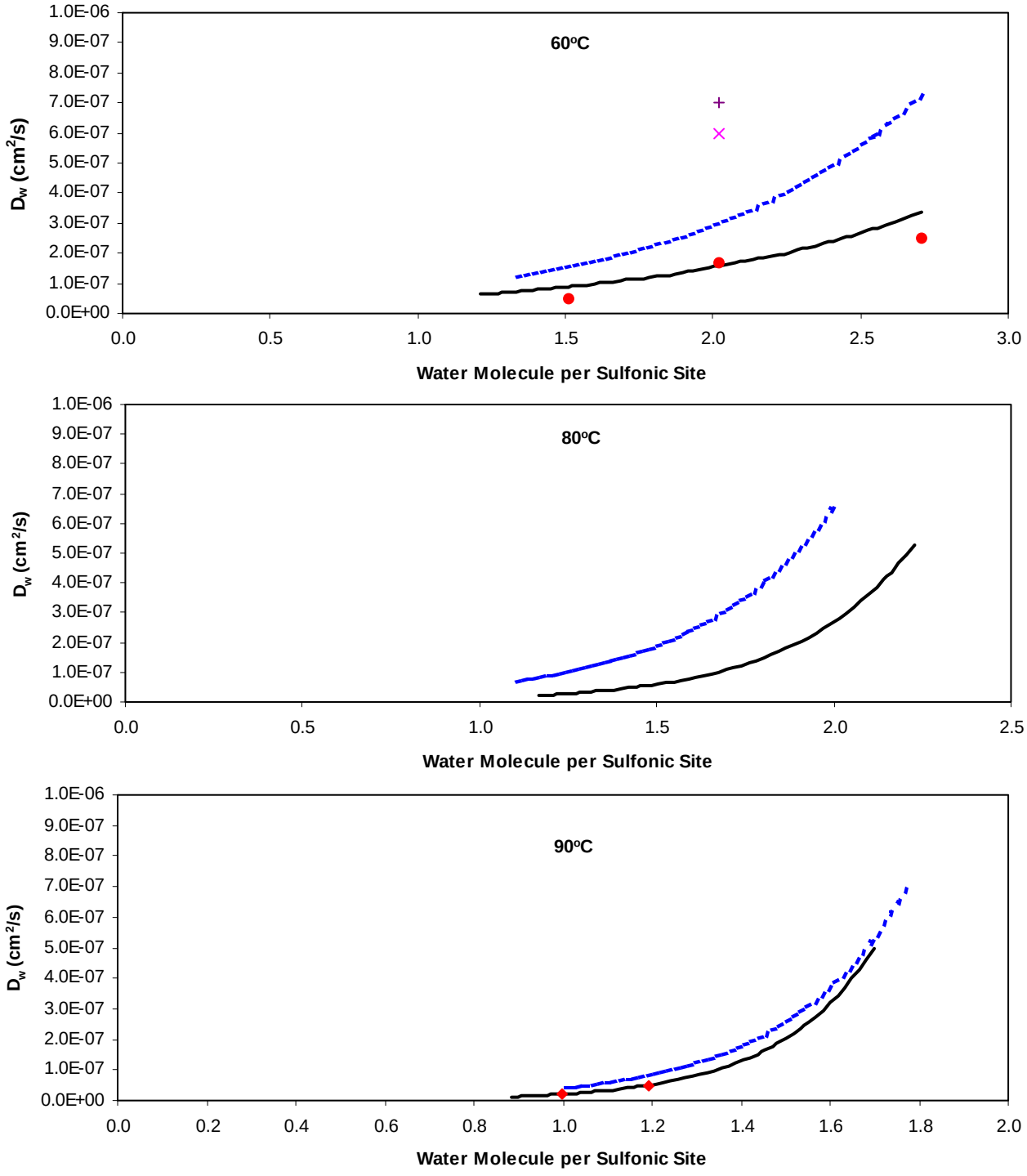

Figure 8. Experimentally fitted effective diffusion coefficient of water in Dow Co. membranes at 60°C, 80°C, and 90°C: (Solid lines) 10.16-μm membrane; (dashed lines) for 17.78-μm membrane. (•) Nafion 117, 50°C, Ref. 11; (x) Nafion 117, 30°C, Ref. 4; (+) Dow XUS 13204.10, 30°C, Ref. 4; (◊) Nafion 117, 100°C, Ref. 11.

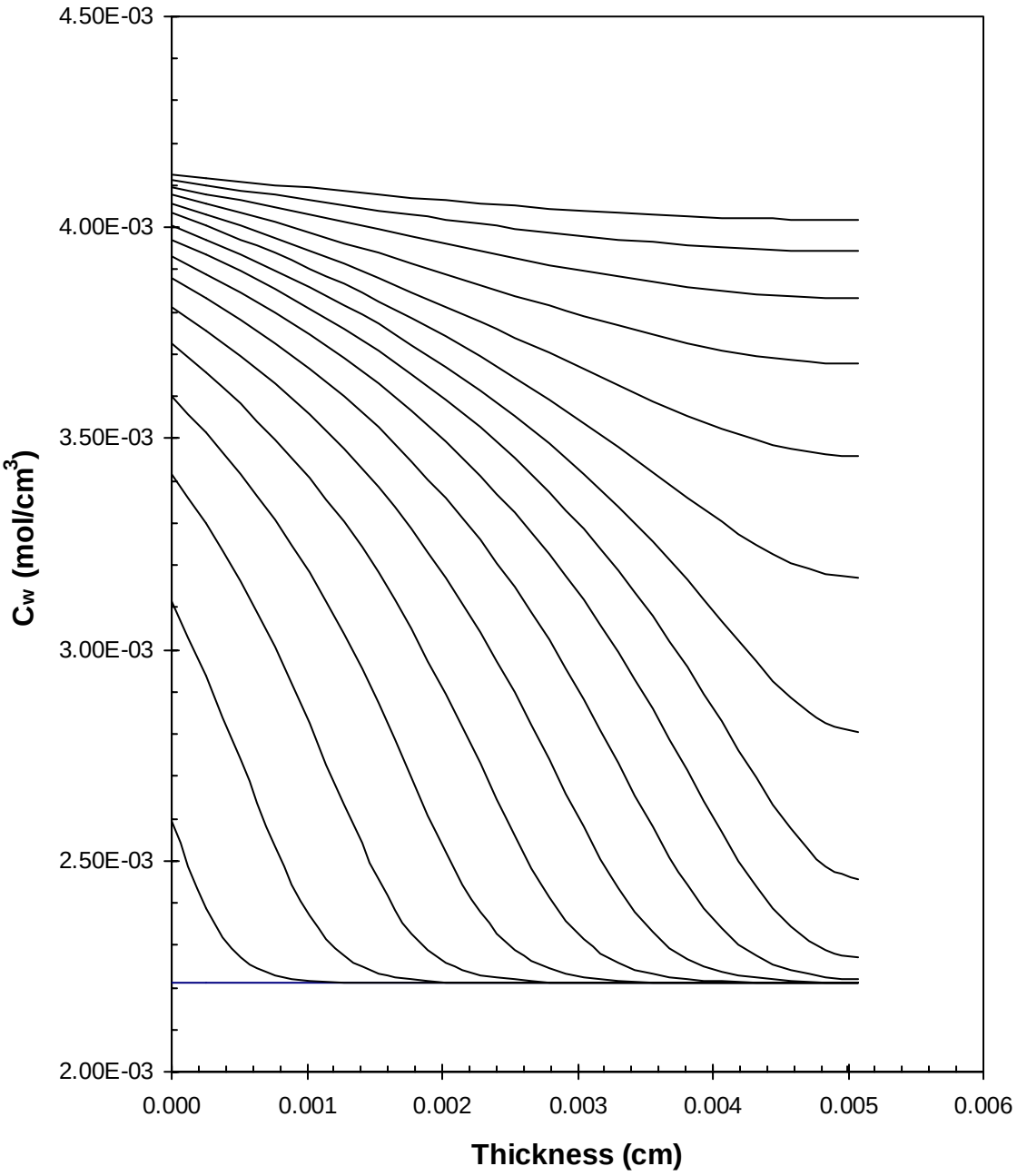

Figure 9. Predicted water distribution in the membrane as a function of time after humidified gas was introduced for 10.16-μm membrane at 90°C. Each line represents a profile every 15-s interval.